International Journal of Innovative Research and Reviews, 8(2) 50-60

International Journal of Innovative Research and Reviews
ISSN: 2636-8919
Website: www.injirr.com

Research paper, Short communication, Review, Technical paper

RESEARCH ARTICLE

Analysis of Heat Transfer in Single-Phase Flow in Circular Mini-Channels

Şendoğan KARAGÖZ[1], Orhan YILDIRIM[1*]

[1] *Department of Mechanical Engineering, Faculty of Engineering, Atatürk University, Erzurum, Türkiye*

* *Corresponding author E-mail: orhan.yildirim@atauni.edu.tr*

ARTICLE INFO

Received : 10.07.2024
Accepted : 12.06.2024
Published : 12.15.2024

***Keywords**:*
MEMS
Pressure Drop
Circular Minichannel
Single-phase
Heat Transfer

ABSTRACT

Due to the increase in heat transfer and the increase in the amount of heat that needs to be removed from the unit area as a result of the reduction in size, this energy needs to be removed. In this study, the effects on heat transfer and friction factor of two circular mini channels with different hydraulic diameters on 6 different flow rates were investigated. Pure water was used as the working fluid and tested at Reynolds numbers ranging from 6000-14000. The experimental results were analyzed and validated using CFD. The Nusselt number and friction factor are analyzed for the results and empirical correlations are proposed. The predictions of heat transfer correlations in mini-channels and classical heat transfer correlations are compared with the experimental results and a high agreement is observed. For the 2.74 mm diameter pipe, the minimum and maximum Nu increase rates compared to 2.26 mm were 30.22% for Re=10724 and 38.33% for Re=13678, respectively. For the 2.26 mm diameter pipe compared to 2.74 mm, the minimum and maximum f increase rates were 31.95% for Re=13678 and 43.10% for Re=10724, respectively. It was found that the reason for the deviation caused by the numerical and experimental results, which are in agreement, is the mismatch in the physical mechanisms affecting the heat and flow transfer.

Contents

1. Introduction

Single-phase heat transfer at the micro-scale has been widely used in industrial and scientific applications, and as a result many papers have been published on the subject in the last two decades. However, there are still inconsistencies between published results and there is no widely accepted model to predict single-phase heat transfer in microchannels. Heat transfer in microchannels has been extensively studied over the past two decades, especially as a result of research aimed at developing effective methods for cooling electronic devices. However, due to the unique characteristics of these

Cite this article Karagöz Ş, Yıldırım O. Analysis of Heat Transfer in Single-Phase Flow in Circular Mini-Channels. *International Journal of Innovative Research and Reviews (INJIRR)* (2024) 8(2) 50-60
Link to this article: http://www.injirr.com/article/view/229

systems, conventional circulation methods are not fully compatible. Therefore, an in-depth investigation of these characteristics is crucial to improve the performance and efficiency of these systems. This study aims to investigate the effects of heat transfer and friction factor on flow rates and entropy production in circular mini-channels with different hydraulic diameters. Furthermore, this study highlights the importance of micro and mini systems in various industries and the ongoing efforts to reduce the size and improve the performance of these systems through micro-electromechanical systems (MEMS) research [1, 2].

For flows in micro channels, Reynolds numbers are normally very low as the flow velocity in little hydraulic diameter is rather small. Because the surface area available for a given flow volume is large, both friction factors and pressure gradients are considerable in microchannel flows. Also, the heat transfer coefficient increases inversely with the tube hydraulic diameter under constant Nusselt number under laminar flow conditions, resulting in a high heat transfer coefficient. Currently, the use of these mini and micro channels, whose hydraulic diameters are very small, is expanding and new research topics are emerging. In some studies, it was found that the transitional and turbulent flow regime in mini and micro channels could not maintain its validity and new correlations were gained in the literature [3]. However, the results obtained in some studies have been found to be in harmony with the basic theories in macro channels, and it has been stated that the basic theories can be applied in channels of these diameters.

Adams et al. [4] examined the effects of forced transport in single-phase turbulent flow in a micro channel with a circular diameter of 0.76-1.09 mm, using water as the flow medium in their research. They compared their results to other studies with Reynolds numbers of 2600-23000 and diameters of 0.102-1.09 mm. They found that the initial values for the Nusselt number (Nu) matched with a difference of ±18.6%. Micro channels, such as microchips, have been shown to be effective in cooling small surfaces of electrical components. These tubes act as a coolant heat exchanger or heat sink. High temperatures can be emitted from different surfaces of the micro channel by natural or forced convection of the liquid flowing in the channel [5, 6]. Steinke and Kandlikar [7] experimentally examined the friction factor for single-phase flow in the micro channel and compared to literature. In their study, they concluded that the friction factor in the micro channel is consistent with basic theories. Van Male et al. [8] used CFD analysis to study the heat and mass properties of flow in silicon square micro channels. The results of the analysis were found to be in agreement with experimental studies and presented mutual equations for different Nu and Sherwood numbers.

In another experiment, a numerical study was conducted to determine the thermal and hydrodynamic characteristics of microchannels in the fixed Re [9]. The study investigated Knudsen number and geometry effects on thermal and hydrodynamic characteristics. As a result of the study, it was observed that the Nu and the friction coefficient fell together with the Knudsen number. It has been reported that the coefficient of heat transfer and friction in the input region is very high, which will drop rapidly as the flow converges to the hydrodynamically fully developed state. In addition, it has been mentioned that viscous diffusion has an important point in determining micro-channel characteristics, and this effect can be more pronounced with the increase in Knudsen number.

Surface roughness is another key consideration when it comes to improving thermal efficiency. Surface walls of microchannels can be smooth or contain tiny features that obstruct flow. The effects of surface roughness on a fully developed, laminar, rough rectangular microchannel were studied using the Gaussian approach in another study [10]. Ho et al. [11] aimed to improve the geometry of minichannel heat sinks in this study on minichannel heat sinks. A comparable study was conducted on the hydrothermal capacities of heat receivers with divergence angles of β=1.38/2.06 degrees in parallel and divergence. The flow rate of the working fluid volumes was determined between 100-600 cm^3 / min under different heat flux densities of 3.2 x 10^4, 4 x 10^4 ve 4.8 x 10^4 W / m Wall temperature distribution of minichannels average number of Nusselts, pressure drop and f related values, thermal resistance of refrigerant and cost of performance (COP) examined the thermal performance under different experimental conditions.

Zhang et al. [12] experimentally examined heat transfer and pressure drop in single-phase flow using micro-fin structure and nanoacluidics, a heat transfer improvement method in a multi-part mini-channel horizontal tube (MMFT). MMFT's are made of parallel rectangular minichannels, and minichannels were designed for use in heat exchanger. One of the improvement techniques was applied and investigated using the amount of heat transfer, the number of Nusselts, and the f and performance evaluation criteria. In this improvement technique five MMFT and three volume concentration nanoacluidics (phi = 0.005%, 0.01% and 0.1%) with different micro fin numbers (n = 0, 1, 2, 3 and 4) were used. In the second stage, the healing technique was applied in combination and experiments were carried out. The number of nusselts increases by 158% at Re=3600, while the performance evaluation criterion reaches 2.0 at Re=5120.

Kim et al. [13, 14] conducted a study to determine the critical channel size and length of minichannels. They have designed a multi-stage minichannel, which uses water chiller as a fluid, with a low pressure drop and to achieve a more efficient cooling rate in a small area. They performed various numerical simulations under single-phase flow and laminar conditions. The diameter of the channel was 2 mm and the length was 530 mm. Analysis were carried out under several parameters including cooling water temperature, channel-wall temperature, mass flux, pressure drop. This numerical work was then compared with experimental results and basic theories were used. Maximum cooling speed in the 5-stage model, the pressure drop was observed to be 40 W/cm^2 at 1383 Pa.

The main aim of this article is to define and verify the validity of the transition and turbulent flow regime in circular cross section mini channel with basic theories [3]. In addition, minichannels are modeled using the finite volume method. The experimental results obtained to validate the numerical model were compared with the CFD results. Thus, the effect of heat transfer and pressure drop in mini-channels was investigated experimentally and numerically.

2. Material and Method

2.1. Experimental method

In the experiments, two pieces of mounting apparatus were produced for mounting the mini-channel to the system. Experiments were carried out on the mini-channels attached to these parts (Figure 1). These parts will not block the flow and aim to ensure that the flow flows smoothly. With these parts installed in the system, a by-pass line was installed to discharge the air in the system. Thanks to the by-pass line, the system is completely filled with water and the overall pressure of the system is fixed at 10 MPa.

[15]The diameter of the pipes used in the test system is 12.7 mm and the pipes used in the test chamber are Cr-Ni (stainless steel 316L) pipes with a diameter of 2.74 mm and 2.26 mm and a length of 37 cm. Experimental studies were carried out at five different Reynolds numbers ranging from 6000-14000 at a flow rate range of 50-60-70-80-90-100 l/h, considering that the inlet temperature was kept constant at 21ºC. The details of the experimental system set up in the laboratory and a schematic diagram of the system are shown in Figure 1 and Figure 2, respectively. The experimental system set up to examine the internal flow in the mini channels consists of a liquid supply section and a test section. Pure water was used as the working fluid. In the experiments, a manual valve was used to adjust the flow rate of the working fluid to achieve the desired Reynolds number and flow rate .

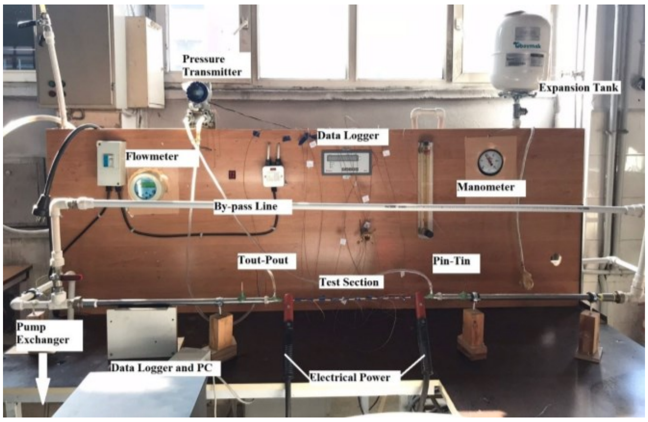

Figure 1 A picture of experimental setup

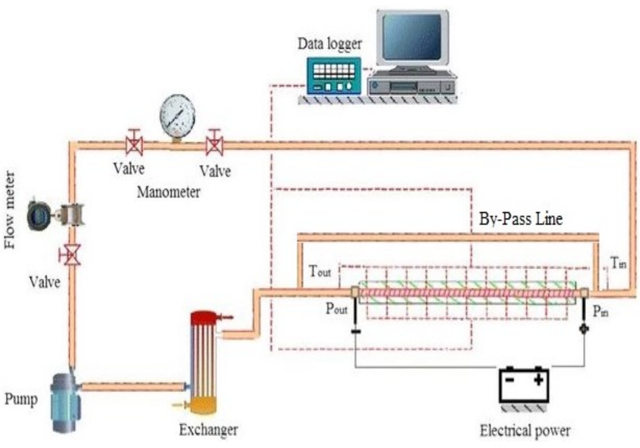

Figure 2 Schematic diagram of the experimental system

The fluid supply section of the system includes a pump to circulate the working fluid, a heat exchanger made of durable material to work under necessary conditions and pressure, a balancing tank, a flow adjustment valve, and a flow meter. This section ensures that the working fluid is brought to the desired inlet conditions. A turbine type flow meter is installed in the system to measure fluid flow. A flow adjustment valve is also added to the system to ensure precise flow measurement [16, 17]. The flow meter is positioned between the balancing tank and the test pipe, with an error rate of ±0.05.

The test area is where single phase flow occurs. It consists of a DC power supply, a fluid inlet control valve, a pressure transducer, a manometer, a test pipe, and thermocouples (Figure 3).

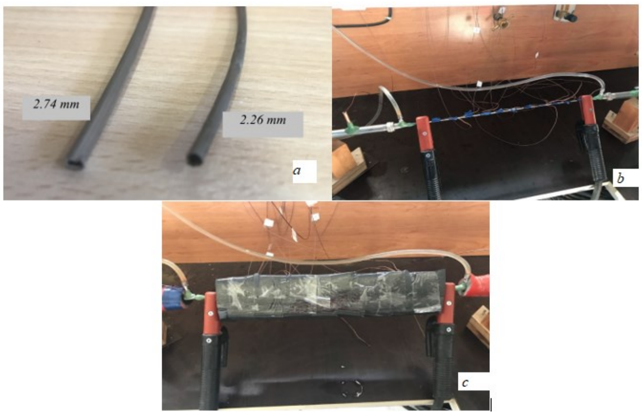

Figure 3 (a)Mini-channels used in the experimental study, (b)Test pipe connections, (c)isolation of test pipe

The test zone was heated by connecting the positive and negative terminals of a DC power supply to both ends of the pipe. The power input used in the experimental system was approximately 24 kW. Temperature measurements were taken using a T-type copper-constantin thermocouple (Figure 4), while system pressure was measured using a pipe-type pressure gauge and pressure losses in the test zone were measured using a pressure transducer. The error rate in the pressure transducer is ±0.01%. The system pressure was maintained at a constant 10 bar and monitored using a Bourdon type pressure gauge, with a reading range of 0.5 bar [18]. Data collected from the test pipe was read and evaluated using an analog/digital data reading card. A total of 11 thermocouples were used in the test zone, with two of them located at the inlet and outlet (Figure 4). The exterior of the test zone was insulated to prevent heat loss (Figure 3c).

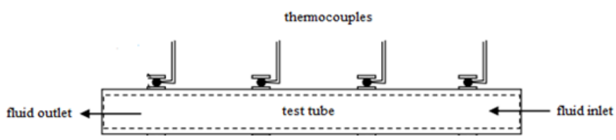

Figure 4 Schematic representation of the connection of thermocouples to the test tube

2.1.1. Computational Fluid Dynamics (CFD) solution

Boundary conditions determined for numerical analysis in the Fluent package program were performed using the given data in the experimental system. The aim of the numerical study is to verify the pipe diameter used in the experimental system and to observe its compatibility with the basic theories. In 3-dimensional analysis, square type mesh was used and boundary layer theory was applied by selecting the infiltration option on the pipe wall. At this stage, the fluid's continuity, momentum, and energy equations were derived using the following assumptions.

- Incompressible fluid
- Fluids have constant physical properties
- Gravity has a negligible influence
- Radiation and viscous heating effects are overlooked
- No-slip condition is taken into account.

In the simulation, a multizone mesh type was used, and the SIMPLE technique was chosen as the solution method for pressure-velocity coupling. In the spatial discretization subset, a second order upwind was used to tackle the problem. ANSYS is used to assess heat and flow attributes utilizing energy equations, as well as continuity and momentum. The CFD software uses a fluid solvent [19]. By keeping the Re between 6000-14000, the k-ε turbulence model was chosen for the solution because the flow was turbulent. In order to obtain reliable calculation results best suited to the thermo-physical properties, k - ε turbulence model with the enhanced wall treatment has been selected. Most importantly, grid independence has been verified by a two-step procedure. all management equations are solved with a control volume scheme [13, 20].

First of all, the continuity, energy and momentum equations are expressed as follows: The conservation of mass principle:

$$\frac{\partial \rho}{\partial t}+\frac{\partial}{\partial x_i}(\rho v_i)=0 \tag{1}$$

Momentum equation:

$$\frac{\partial}{\partial x_j}(\rho u_i u_j)=-\frac{\partial P}{\partial x_i}+\frac{\partial}{\partial x_j}[\mu\left(\frac{\partial u_i}{\partial x_j}+\frac{\partial u_j}{\partial x_i}\right)] + \frac{\partial}{\partial x_j}(-\rho\overline{u_i' u_j'}) \tag{2}$$

where the working fluid viscosity, fluctuating velocity, and axial velocity components are, μ , u', and u_j respectively. The term $\rho\overline{u_i' u_j'}$ stands for turbulent shear stress, also known as Reynolds stress.

The law of energy conservation:

$$\frac{\partial}{\partial t}(\rho e)+\frac{\partial}{\partial x_j}(\rho v_j c_p T-k\frac{\partial T}{\partial x_j}) = u_j\frac{\partial p}{\partial x_j}+[\mu((\frac{\partial v_i}{\partial x_j}+\frac{\partial v_j}{\partial v_i}) -\frac{2}{3}\frac{\partial v_k}{\partial x_k}\delta_{ij})] \tag{3}$$

ρ density, μ dynamic viscosity, u velocity, T temperature, P pressure and Cp specific heat coefficient. Water was used as the fluid flowing in a stainless steel pipe and the system was simulated in a steady state.

The k turbulence model with increased wall treatment is used for numerical simulation in this study:

$$\frac{\partial}{\partial t}(\rho k)+\frac{\partial}{\partial x_i}(\rho k v_i) = \frac{\partial}{\partial x_j}[(\frac{\mu+\mu_t}{\sigma_k})\frac{\partial k}{\partial x_j}]+\mu_t(\frac{\partial v_i}{\partial x_j} + \frac{\partial v_j}{\partial v_i})\frac{\partial v_i}{\partial x_j}-\rho\varepsilon \tag{4}$$

$$\frac{\partial}{\partial t}(\rho \varepsilon)+\frac{\partial}{\partial x_i}(\rho \varepsilon v_i) = \frac{\partial}{\partial x_j}[(\frac{\mu+\mu_t}{\sigma_\varepsilon})\frac{\partial \varepsilon}{\partial x_j}] + C_{1\varepsilon}\frac{\varepsilon}{k}\mu_t(\frac{\partial v_i}{\partial v_j}+\frac{\partial v_j}{\partial v_i})\frac{\partial v_i}{\partial v_j} - C_{2\varepsilon}\rho\frac{\varepsilon^2}{k}-\alpha\rho\frac{\varepsilon^2}{k} \tag{5}$$

$$\mu_t=\rho C_\mu\frac{k^2}{\varepsilon} \tag{6}$$

The turbulent kinetic energy generation and dissipation rates are given by Γ_k and ε, respectively. The following empirical constants are used to calculate the realizable k- ε turbulence model:

$C_{1\varepsilon}=1.44, C_{2\varepsilon}=1.90, \sigma_k=1.0, \sigma_\varepsilon=1.2.$

Figure 5 shows the three-dimensional geometry, including the model and boundary conditions.

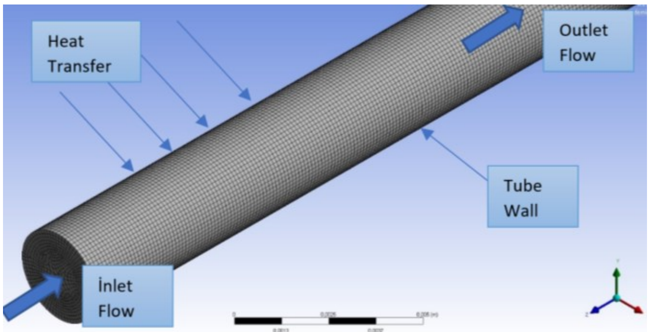

Figure 5 A schematic representation of the mesh quality and boundary condition

The CFD simulation was performed on small cells to accurately capture the pressure gradient, boundary layer, and small size of the mini-channels. Analytical solutions were used to validate the results, compare them with experimental data and ensure a high level of agreement. The simulation converged at 400 iterations. To reduce uncertainty, the boundary conditions, such as fluid inlet temperature, pressure at the pipe outlet, pipe length and diameter, and Reynolds number range were carefully studied and defined. The solution is considered to be converged sufficiently when the normalized residual of 10^{-5} for momentum and mass and 10^{-7} for energy equations.

2.1.2. Experimental Calculation

Using the obtained experimental data Nu, f , and Re is calculated. Accordingly, the heat given to the system, DC power volt and current of the source directly has been read. Heat from power source losses occurred while transferring to the fluid. This $\sqrt{3}$ to prevent and account for losses multiplied by the coefficient. From here to the system amount of heat supplied [21];

$$Q = VI\sqrt{3} \tag{7}$$

Losses from the system can be caused by radiation from the surface or by transmission from the surface of the pipe to the surrounding environment. The literature also states that when the test zone is well insulated in the system, its losses with radiation can be neglected. Heat losses by conduction can be determined by measuring the average surface temperature of the pipe and the outer surface temperature of the insulation material. Using measured temperatures, convection coefficient(h) can be determined as follows [22];

$$h = \frac{Q}{A(T_w - (T_{in} + T_{out})/2} \tag{8}$$

The calculated heat transfer coefficient (h) will help us find the Nu. In internal flows, friction of the fluid causes pressure drop. The pressure drop, which is a function of the classical f, is practically expressed in the following equation [15–17].

$$Nu = \frac{hD}{k} \tag{9}$$

$$\Delta P = f\frac{L}{D}\left(\frac{1}{2}\rho V^2\right) \tag{10}$$

The Re is calculated using the total flow rate at the inlet section as follows:

$$Re = \frac{\rho VD}{\mu} \tag{11}$$

The values obtained for the Nu and f of the straight pipe are examined for validation test results by comparing CFD and earlier correlations analysis under comparable conditions.

Where, L Length of the tube (m),f Friction factor, ***D*** Pipe inside diameter (m), ***ΔP*** Pressure drop (bar) ,***Re*** Reynolds number, Q˙ Heat transfer (W), T_w average surface temperature, T_{in} pipe inlet temperature, T_{out} pipe outlet temperature, ***μ*** Dynamic viscosity (kg/ms), ***in*** Inlet, ***out*** Outlet, ***ρ*** Density (kg/m3), ***v*** Velocity (m/s), ***k*** Thermal conductivity of fluid (W/m K), defined as.

3. Research Findings and Discussion

3.1. Comparison experimental results

The data obtained at the end of the experimental and numerical study were evaluated and the results were given graphically.

The results of the study show that when single phase flow is present in mini-channels with diameters of 2.74 mm and 2.26 mm, the Nusselt number (Nu) increases with an increase in the Reynolds number, which is in agreement with the basic theories. This is demonstrated in Figure 6, which presents the experimental results obtained in the study [23, 24]. The Nu number correlation obtained for the operating conditions in mini-channels with a diameter of 2.74 mm is $Nu=0.038.Re^{0.79}.Pr^{1/3}$.

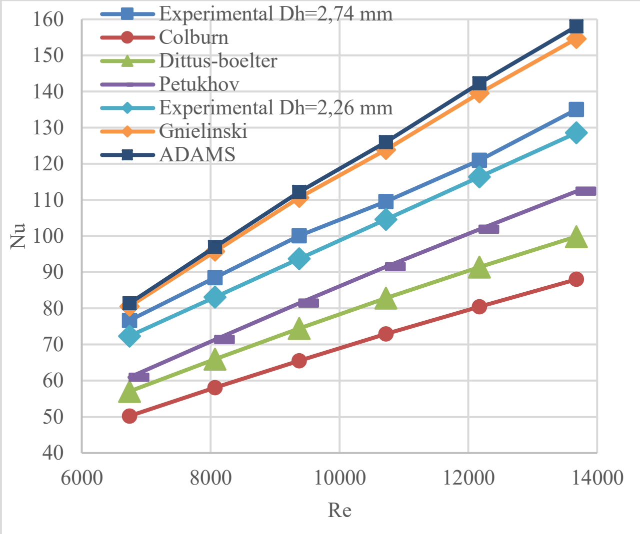

Figure 6 Nu-Re exchange in mini channels

Similarly, for the mini-channel with a diameter of 2.26 mm, the Nu number correlation obtained is $Nu=0.030.Re^{0.81}.Pr^{1/3}$. For the 2.74 mm diameter pipe, the minimum and maximum Nu increase rates compared to 2.26 mm were 30.22% for Re=10724 and 38.33% for Re=13678, respectively.

When these correlations were compared to the basic theories such as Colburn and Dittus-Boelter Correlation, it was found that they were in agreement [22]. The reduction in diameter in mini-channels was found to approach the basic theories more closely. These results indicate that the correlations obtained in this study provide a new contribution to the literature on heat transfer in mini-channels and may be useful for predicting heat transfer in mini-channels under similar conditions.

Colburn Correlation;

$$Nu = 0{,}023.Re^{0{,}8}.Pr^{1/3} \tag{12}$$

Dittus-Boelter Correlation;

$$Nu = 0{,}023.Re^{0{,}8}.Pr^{n} \tag{13}$$

Gnielinski Correlation;

$$\mathrm{Nu} = \frac{(f/8)(\mathrm{Re}-1000)\mathrm{Pr}}{1+12.7(f/8)^{0.5}(\mathrm{Pr}^{2/3}-1)} \mathrm{for} 3x10^3 < \mathrm{Re} < 5x10^6 \tag{14}$$

Petukhov Correlation:

$$\mathrm{Nu} = \frac{(f/8)\mathrm{RePr}}{1.07+12.7(f/8)^{0.5}(\mathrm{Pr}^{2/3}-1)} \mathrm{for} 10^4 < \mathrm{Re} < 5x10^6 \tag{15}$$

Adams Correlation:

$$Nu_{GN} = \frac{\left(\frac{f}{8}\right)(Re-1000).Pr}{1+12{,}7(\frac{f}{8})^{\frac{1}{2}}[Pr^{\frac{2}{3}}-1]} \; 3x10^3 < Re < 5x10^6 \tag{16}$$

The results of this study, as shown in Figure 7, indicate that the friction factor (f) decreases as the Reynolds number (Re) increases, in agreement with the basic theories in the literature for single phase flow in mini-channels with diameters of 2.74 mm and 2.26 mm. It is observed that the initial values of the friction coefficient were high.

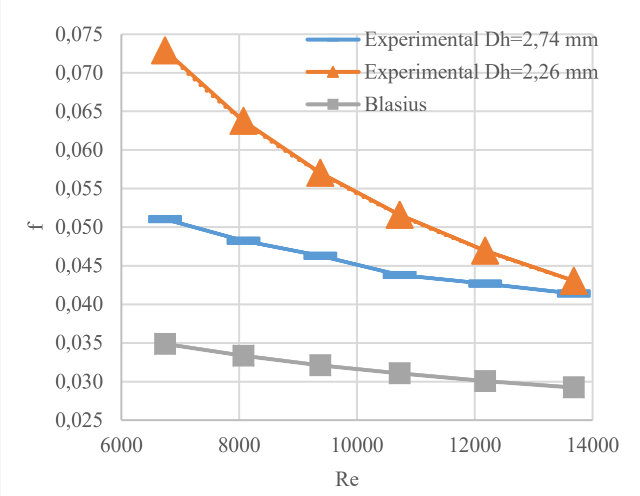

Figure 7 f-Re change in mini channels

This may be due to the fact that the pressure drop values cannot be accurately measured at low speeds, resulting in the friction coefficient values obtained from experimental studies in mini and micro channels to differ from the expected values as reported in previous studies [25, 26]. The correlation of the friction factor obtained for operating conditions in mini-channels with a diameter of 2.74 mm is f= 51,442. $Re^{-0,744}$. The correlation for the mini-channel with a diameter of 2.26 mm is f= 0,7222. $Re^{-0,301}$. In previous studies, it has been observed that the friction coefficient value in the turbulent region is higher than the basic theories [25]. Recent studies have suggested that the friction coefficient can be reduced by modifying the channel geometry, surface properties, and fluid interactions [27, 28]. For the 2.26 mm diameter pipe compared to 2.74 mm, the minimum and maximum f increase rates were 31.95% for Re=13678 and 43.10% for Re=10724, respectively.

Blasius equation;

$$f = 0.3164/\mathrm{Re}^{0.25} \text{ for } \mathrm{Re} \leq 5x10^5 \tag{17}$$

3.2. Comparison of experimental and numerical results

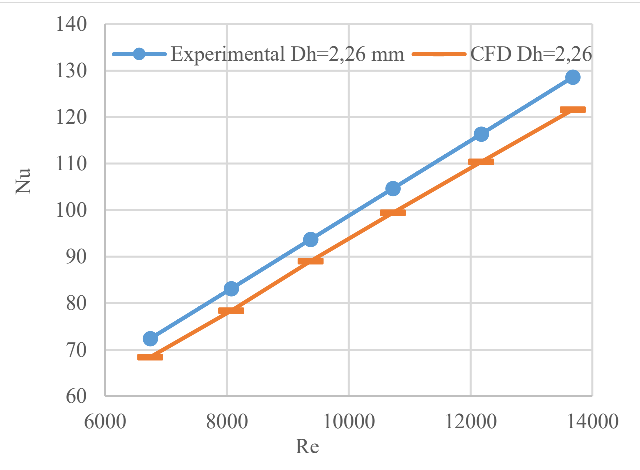

Figure 8 Nu-Re Relationship in Experimental and Numerical Studies in the Mini-channel with a diameter of 2.26 mm.

The results of the study, as shown in Figure 8, Figure 9 and Figure 10, indicate that the Nusselt number (Nu) versus Reynolds number (Re) relationship of experimental and numerical results in single-phase flow in mini-channels with diameters of 2.74 mm and 2.26 mm were compared.

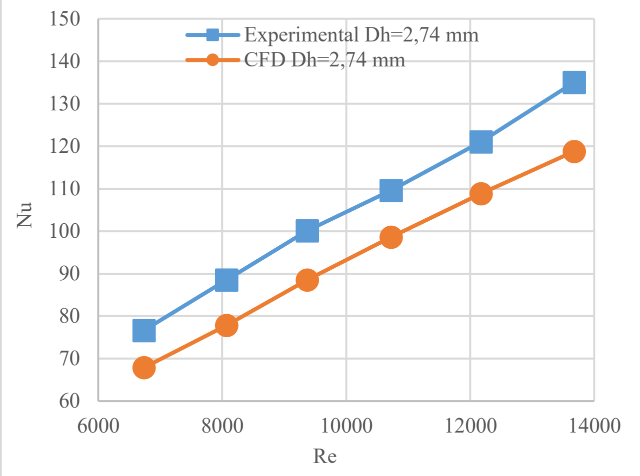

Figure 9 Nu-Re Relationship in Experimental and Numerical Studies in the Mini-channel with a diameter of 2.74 mm.

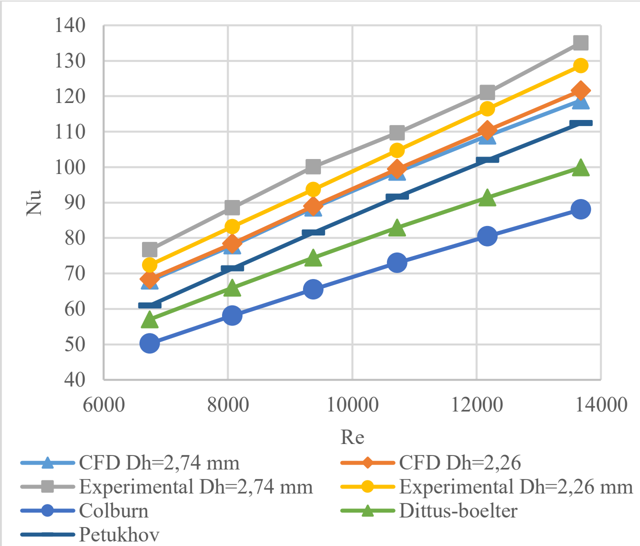

Figure 10 Comparison of experimental and numerical results in mini channels with basic theories and Nu-Re relationship

By examining the figures, it can be seen that the values obtained from numerical solutions and the values obtained from experimental work are in close agreement. In the numerical analysis, it was observed that the difference between the numerical and experimental results is expected to occur due to the use of equations for fluid continuity, momentum, and energy that are similar to those used in macro channels, but these equations do not take into account the limit condition of no-slip at the wall in mini channels. As the diameter and pressure decrease in mini channels, the wall slip increases, which leads to an increase in fluid particle movement and transport in the wall. This is in agreement with the findings of Adams et al. [4] which state that the results obtained from experimental studies in turbulent flow in mini-channels are higher than the values obtained from basic theories and numerical solutions. It is also noted that the average heat transfer coefficient values for the channel diameter of 2.26 mm are higher than the channel diameter of 2.74 mm. Therefore, the average heat transfer coefficient increases as the diameter of the channel decreases, as previously reported by Ghasemi [29].

It was observed that the results obtained from numerical analysis were close to each other and in harmony with the experimental value. The number of Re increases to a certain extent greater than the numerical values [18, 26]. At diameters 1 mm and below the diameter, it was stated that FLUENT results using conservation equations used in macro pipes in turbulent flow decreased by 40% or higher than experimental values with an error increasing with a shrinking diameter.

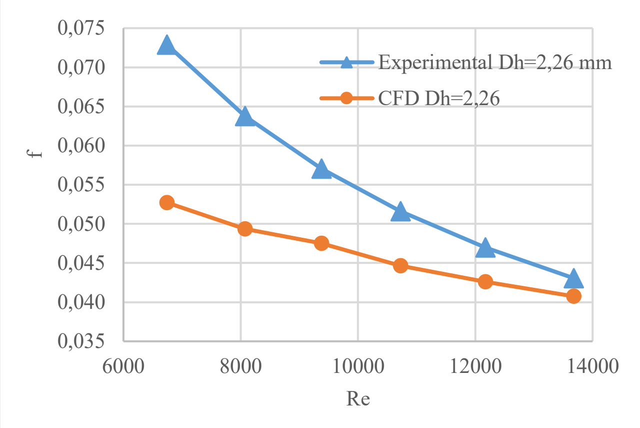

Figure 11 f-Re relation in experimental and numerical studies in diameter 2.26 mm Minichannel

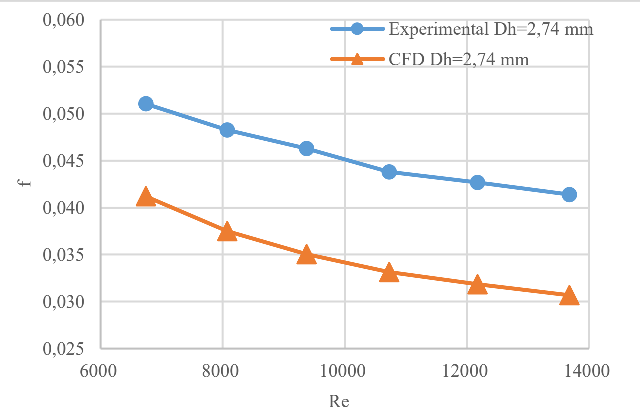

Figure 12 f-Re relation in experimental and numerical studies in diameter 2.74 mm Minichannel

The results of the study, as shown in Figure 11 and Figure 12, indicate that the friction factor (f) versus Reynolds number (Re) relationship in experimental and numerical results made in the mini-channel are in agreement. Figure 11 and Figure 12 show that the numerical results are consistent with the literature, and are in harmony with the experimental results. The results show that as the Reynolds number increases, the coefficient of friction decreases. It is observed that the friction factor calculated by CFD is lower than the experimental results when the Reynolds number is low.

The results of this study, as shown in Figure 11, Figure 12, and Figure 13, indicate that the friction factor (f) versus Reynolds number (Re) relationship of experimental and numerical results in single-phase flow in mini-channels with diameters of 2.74 mm and 2.26 mm was compared.

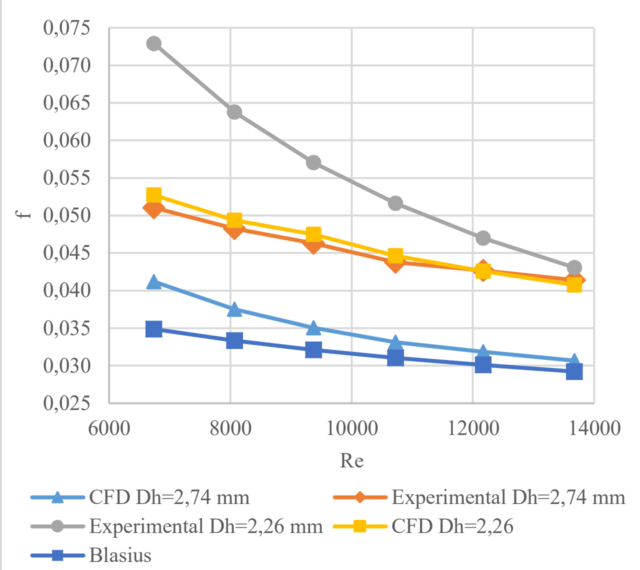

Figure 13 Comparison of experimental and numerical results in Minichannels with basic theories, f-Re relationship

It has been observed that the numerical results in the turbulent flow region give greater values than basic theories, and experimental results obtained in mini-channels also increase steadily as the diameter decreases. This difference appears to increase more as the Reynolds number increases. The channel with a larger diameter shows a lower pressure drop. As the channel diameter increases, the cross-sectional area increases and the speed decreases, hence the pressure drop decreases, as reported by Compell and Kandlikar [30]. They stated in an experimental study that the coefficient of friction obtained in laminar flow within the channel is close to conventional values. Steinke and Kandlikar [7] discussed studies on the coefficient of friction in flows with different Reynolds numbers in channels with different hydraulic diameters and created a data pool. They also calculated the coefficient of friction in the laminar and turbulent region using basic theories and compared these values to the results obtained by experimental correlations. They used the Blasius equation in the turbulent region. As can be seen in Figure 11, Figure 12, and Figure 13, the reason why experimental and numerical results differ is explained by the decrease in diameter and pressure in mini-channels. As the Reynolds number increases, the coefficient of friction appears to get closer to the basic theories as the diameter grows, but as the diameter decreases, this ratio increases more.

In the numerical analysis performed in this study, the k-ε standard model was used as the solution method. This method is closely related to the iteration process, and it was observed at which iteration the solution becomes stable. In a converged solution that is independent of the number of iterations, it must remain constant for all variables or constantly decrease, and the values must remain constant after a certain point. The results showed that the convergence did not change as the number of iterations increased. This suggests that the numerical model used was able to accurately predict the heat transfer and pressure drop in the mini-channels under study.

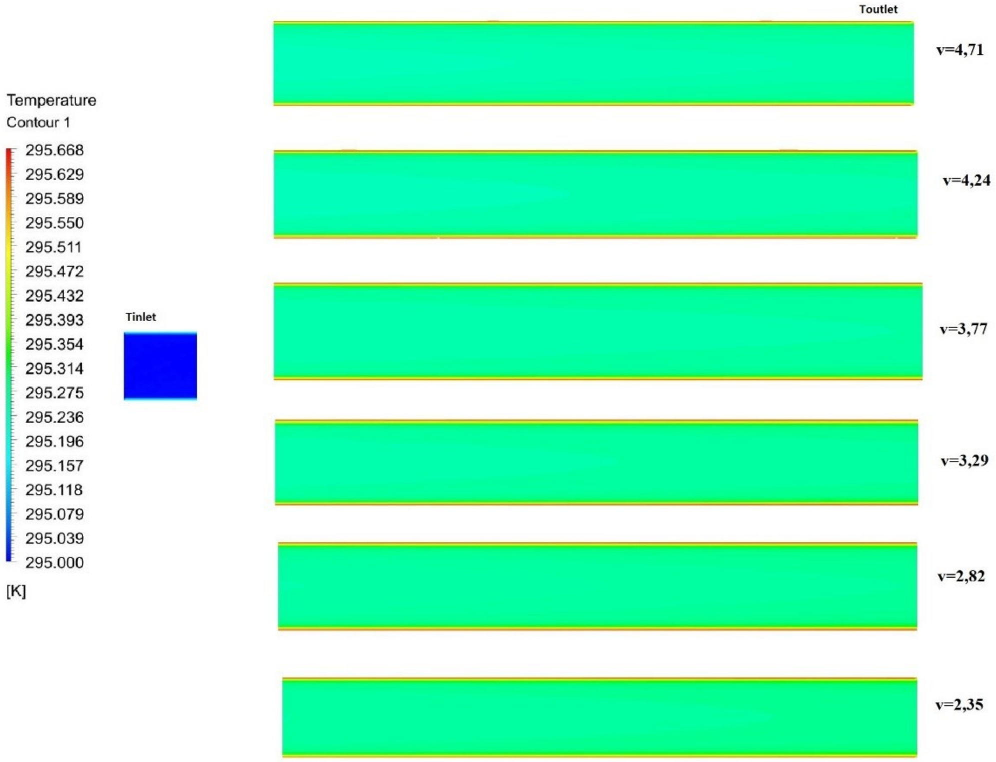

Figure 14 Temperature distribution at the inlet and outlet of the channel as a result of numerical analysis on the 2.74 mm Minichannel

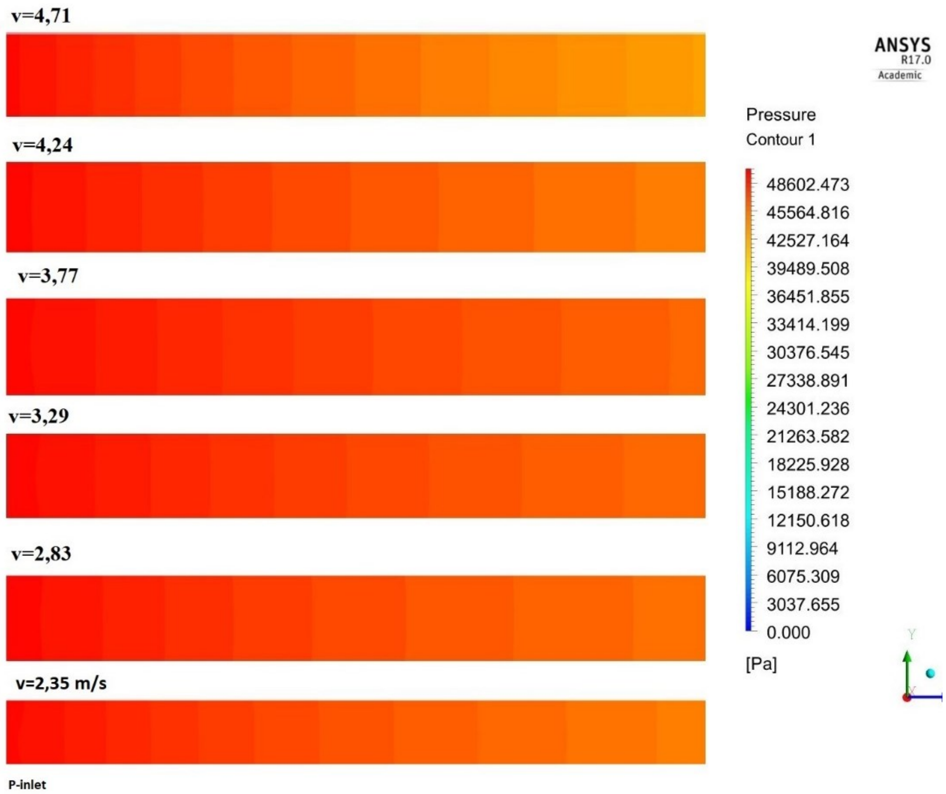

Figure 15 Pressure distribution at the inlet of the channel as a result of the numerical analysis in the 2.74 mm Mini channel

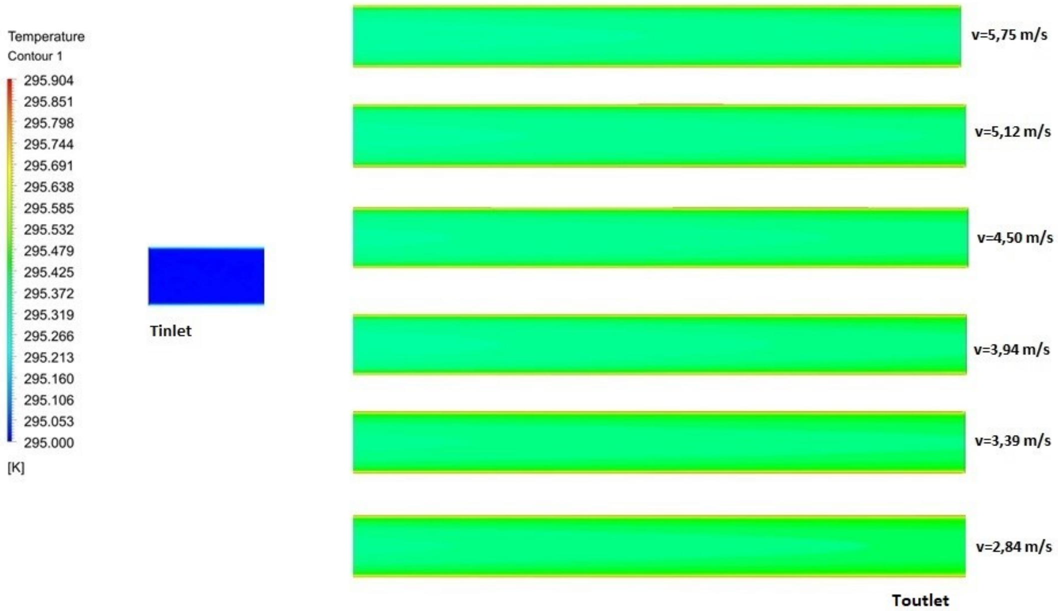

Figure 16 Temperature distribution at the entrance and exit of the channel as a result of numerical analysis in the 2.26 mm Mini channel

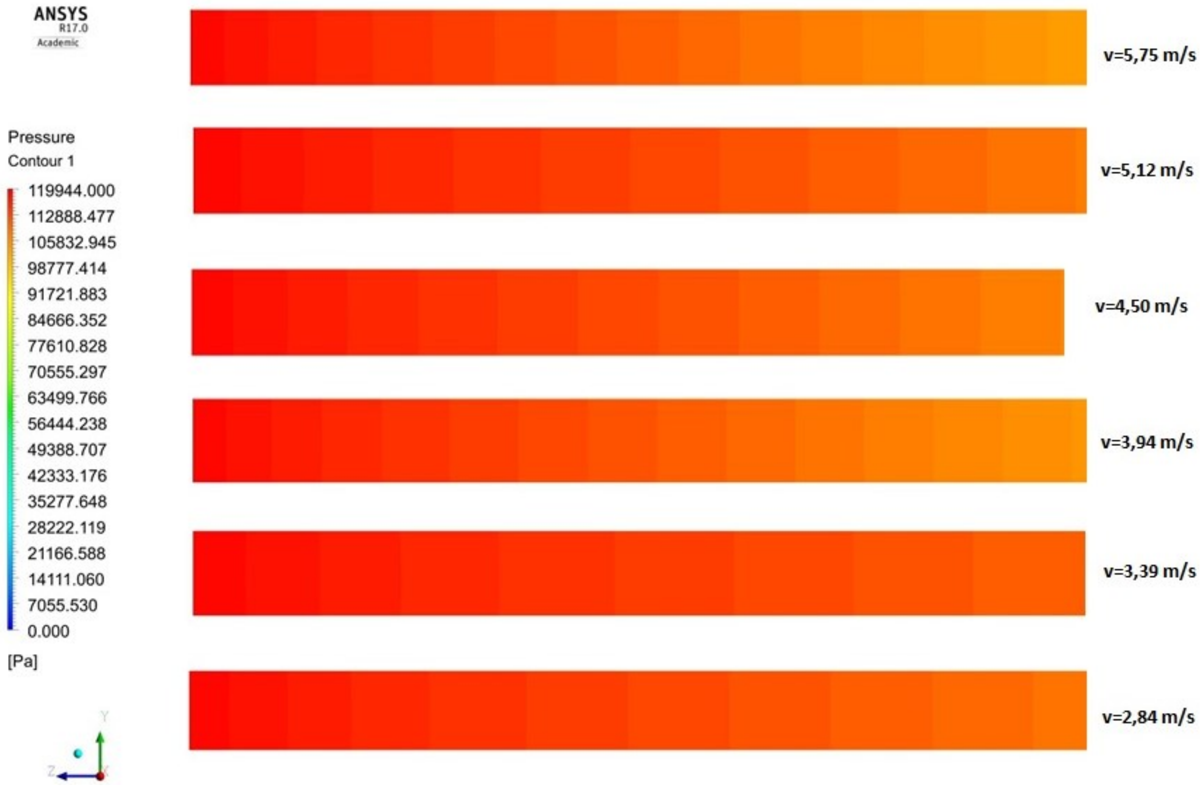

Figure 17 Pressure distribution at the inlet of the channel as a result of the numerical analysis of the 2.26 mm Mini channel

It should be noted that the calculation of the above hydrodynamic entrance length is based on a uniform inlet velocity profile (Figure 14-Figure 17). In microchannel coolers, the flow encounters sudden contraction at the inlet and expansion at the outlet. For such conditions, Rohsenow et al. [31] have argued that it is necessary to assume that the inlet state is hydrodynamically fully developed but thermally developing due to the effects of the sudden contraction at the inlet. As shown in Figure 10, experimental Nusselt numbers are generally higher in this turbulent region than the predictions from the correlations in [4, 32, 33]. On the other hand, the predictions from Petukhov and Dittus-Boelter correlations [22], which are likely to be for fully turbulent flow (Re > 3000), cover a more turbulent regime than the results obtained in this study. It can be noted that the effects of the entrance length have not been included in any of the turbulent flow correlations; while entrance length effects are less important in turbulent flow, it may still contribute to the observed inconsistencies. However, the slope of the variation of the Nusselt number with Reynolds number is consistent with the slopes predicted by Dittus-Boelter and Gnielinski correlations. Further results in the turbulent region are needed to address this issue and identify predictive correlations suitable for this regime. The good agreement between the experimental and simulation results suggests that a conventional computational analysis approach can predict the heat transfer behavior in microchannels of the dimensions considered here.

4. Conclusion

In this experimental and numerical study, the heat transfer and pressure drop characteristics of turbulent flow in mini-channels of different diameters were investigated. Using mini-channels of two different diameters and 6 different flow rates, experiments were conducted under constant heat flux conditions, and the Nusselt number (Nu) and friction factor (f) were determined from the obtained data. Additionally, numerical simulations were performed using CFD and the results were compared to the experimental data to validate both the numerical model and the experimental measurements.

The results of the study showed that the heat transfer coefficients and Nu for water flowing through channels with diameters of 2.74 and 2.26 mm were higher than predicted by traditional correlations such as Colburn, Dittus-Bolter, and Gnielinski [32]. For the 2.74 mm diameter pipe, the minimum and maximum Nu increase rates compared to 2.26 mm were 30.22% for Re=10724 and 38.33% for Re=13678, respectively. For the 2.26 mm diameter pipe compared to 2.74 mm, the minimum and maximum f increase rates were 31.95% for Re=13678 and 43.10% for Re=10724, respectively. A comparison of the experimental and numerical results with those reported in previous studies revealed that the trends in heat transfer enhancement were consistent. In turbulent flow, the f values obtained from traditional correlations for macro dimensions gave small errors for the diameters studied. It was also observed that numerical method equations based on conservation equations for macro dimensions were in good agreement with the experimental values when the diameter is larger and the Reynolds number is smaller. However, with smaller diameters and higher Reynolds numbers, the numerical method results were found to be smaller than the experimental values. Furthermore, it was observed that in turbulent flow, if the hydraulic diameter (Dh) is larger than 1 mm, the Nu values obtained from basic theories in macro dimensions are smaller than the experimental results. The obtained equations were found to make a new contribution to the literature on mini-channels, and the study also found that mini-channels have smaller friction force than macro pipes, and that as the diameter decreases in mini-channels, the heat transfer coefficient increases more. The study also found that the difference between the f factors increases as the diameter of the mini-channels decreases, and that this difference becomes more pronounced as the Reynolds number increases. The reasons for the differences between numerical and experimental results in the f-Re relationship were found to be related to diameter reduction and pressure drop. As the Reynolds number increases, the coefficient of friction appears to get closer to the basic theories as the diameter grows, but as the diameter decreases, this ratio increases more

Acknowledgements

This work was carried out by Ataturk University Scientific Research Projects Coordination Unit Grant No. Supported by 2016-205. We would like to thank Atatürk University Rectorate for research support.

Conflict of Interest

The authors declare that they have no known competing financial interests or personal relationships that could have appeared to influence the work reported in this paper.

References

[1] Kandlikar SG, Grande WJ. Evolution of Microchannel Flow Passages–Thermohydraulic Performance and Fabrication Technology. *Heat transfer engineering* (2003) **24**(1):3–17. doi:10.1080/01457630304040.

[2] Tabeling P. *Introduction to microfluidics*: OUP Oxford (2005).

[3] Jokar A, Eckels SJ, Hosni MH. Single-phase flow in meso-channel compact heat exchangers for air conditioning applications. *Heat transfer engineering* (2010) **31**(1):3–16. doi:10.1080/01457630903263200.

[4] Adams TM, Abdel-Khalik SI, Jeter SM, Qureshi ZH. An Experimental Investigation of Single-Phase Forced Convection in Microchannels. *International Journal of Heat and Mass* (1998) **Transfer,.41(6–7**:851–857. doi:10.1016/S0017-9310(97)00180-4.

[5] Krishnan R, A. C, H. Z, Na H, Lee HJ. Experimental investigation on critical heat flux measurement in parallel microchannel heat sink at low mass fluxes. *Journal of Mechanical Science and Technology* (2021) **35**(7):3211–3221. doi:10.1007/s12206-021-0641-x.

[6] Zhong X, Wang T, Liu J, Zhang Y, Cheng Z. Computational Fluid Dynamics Simulation for On-Chip Cooling with Carbon Nanotube Micro-Fin Architectures. In: *International Conference on Electronic Materials and Packaging. IEEE* (2006). p. 1–6.

[7] Steinke ME, Kandlikar SG. Single-Phase Liquid Friction Factors in Microchannels. In: *3rd International Conference on Microchannels and Minichannels Conference*. Univ Toronto, Toronto, CANADA (2005). p. 1073–1083.

[8] Male P, Croon M, Tiggelaar RM, Berg A, Schouten JC. Heat and mass transfer in a square microchannel with asymmetric heating. *International journal of heat and mass transfer* (2004) **47**(1):87–99. doi:10.1016/S0017-9310(03)00401-0.

[9] Shokouhmand H, Bigham S. Slip-flow and heat transfer of gaseous flows in the entrance of a wavy microchannel. *International Communicationsin Heat and Mass Transfer* (2010) **37**:695–702. doi:10.1016/j.icheatmasstransfer.2010.03.008.

[10] Shokouhmand H, Aghvami M, Afshin MJ. Pressure Drop and Heat Transfer of Fully Developed, Laminar Flow in Rough, Rectangular Microchannels. *International Conference on Nanochannels, Microchannels, and Minichannels* (2008) **48345**:153–157.

[11] Ho CJ, Chang PC, Yan WM, Amani P. Thermal and hydrodynamic characteristics of divergent rectangular minichannel heat sinks. *International journal of heat and mass transfer* (2018) **122**:264–274. doi:10.1016/j.ijheatmasstransfer.2018.01.122.

[12] Zhang J, Diao Y, Zhao Y, Zhang Y. An experimental investigation of heat transfer enhancement in minichannel: Combination of nanofluid and micro fin structure techniques. *Experimental Thermal and Fluid Science* (2017) **81**:21–32. doi:10.1016/j.expthermflusci.2016.10.001.

[13] Kim Y, Kim M, Ahn C, Kim HU, Kang SW, Kim T. Numerical study on heat transfer and pressure drop in laminar-flow multistage mini-channel heat sink. *International journal of heat and mass transfer* **108**:1197–1206. doi:10.1016/j.ijheatmasstransfer.2016.12.025.

[14] Kim B. An experimental study on fully developed laminar flow and heat transfer in rectangular microchannels. *International Journal of*

Heat and Fluid Flow (2016) **62**:224–232. doi:10.1016/j.ijheatfluidflow.2016.10.007.
[15] Firat I, Karagoz S, Yildirim O, Yilmaz M. Performance and entropy production analysis of angle blade turbulators used to increase heat transfer. *Journal of Thermal Analysis and Calorimetry* (2023) **148**(15):7811–7828.
[16] Karagoz S, Erzincanli S, Yildirim O, Firat I, Kaya M, Comakli O, et al. Experimental investigation of the effect of wave turbulators on heat transfer in pipes. *Thermal Science* (2022) **26**(2 Part C):1771–1783.
[17] Firat I, Karagoz S, Yildirim O, Sonmez F. Experimental investigation of the thermal performance effects of turbulators with different fin angles in a circular pipe. *International Journal of Thermal Sciences* (2023) **184**:107969.
[18] Karagoz S, Afshari F, Yildirim O. Experimental and numerical investigation of the cylindrical blade tube inserts effect on the heat transfer enhancement in the horizontal pipe exchangers. *Heat and Mass Transfer* (2017) **53**:2769–2784. doi:10.1007/s00231-017-2021-8.
[19] Workbench A. *Fluent software* (version 17.2).
[20] Afshari F, Ghasemi Zavaragh H, Nicola G. Numerical analysis of ball-type turbulators in tube heat exchangers with computational fluid dynamic simulations. *International journal of environmental science and technology* (2019) **16**:3771–3780. doi:10.1007/s13762-018-2012-4.
[21] Iprocessmart (2017). Available from: https://www.iprocessmart.com/techsmart/3-phase_equations.htm,
[22] Cengel YA, Boles MA. *Thermodynamics: An Engineering Approach*: McGraw-Hill Education, OH (2002).
[23] Eiamsa-Ard. S, Thianpong C, Eiamsa-ard P. Turbulent heat transfer enhancement by counter/co-swirling flow in a tube fitted with twin twisted tapes. *Experimental Thermal and Fluid Science* (2010) **34(1**:53–62. doi:10.1016/j.expthermflusci.2009.09.002.
[24] Eiamsa-Ard. S, Thianpong. C, P. E, Promvonge P. Thermal characteristics in a heat exchanger tube fitted with dual twisted tape elements in tandem. *International Communications in Heat and Mass Transfer* (2010) **37(1**:39–46. doi:10.1016/j.icheatmasstransfer.2009.08.010.
[25] Hrnjak P, Tu X. Single phase pressure drop in microchannels. *International Journal of Heat and Fluid Flow* (2007) **28**(1):2–14. doi:10.1016/j.ijheatfluidflow.2006.05.005.
[26] Deniz E. *Numerical Investigation of Flow and Heat Transfer in Mini Channels, Master Thesis*: Istanbul Technical University, Institute of Science and Technology. Turkey (2007).
[27] Garimella SV. Singhal, V.,(2004) Single-Phase Flow and Heat Transport and Pumping Considerations in Microchannel Heat Sinks. *Heat transfer engineering* **25**:1,15–25.
[28] Şara ON, Yapici S. Pressure Drop and Heat/Mass Transfer in Micro Channels: I-Pressure Drop and Friction Factor Relations. *Engineer and Machine* (2007) **48**:570.
[29] Ghasemi SE, Ranjbar AA, Hosseini MJ. Experimental and numerical investigation of circular minichannel heat sinks with various hydraulic diameter for electronic cooling application. *Microelectronics Reliability* (2017) **73**:97–105. doi:10.1016/j.microrel.2017.04.028.
[30] Compbell LA, Kandlikar SG. Effects of Entrance Condition of Frictional Losses and Transition to Turbulance. In: *Proceedings of IMECE'02*. New Orleans, LA (2002).
[31] Rohsenow WM. *Handbook of heat transfer*. New York: McGraw-Hill (1998).
[32] Gnielinski V. New equations for heat and mass transfer in turbulent pipe and channel flow. *Int. Chem. Eng* (1976) **16**(2):359–368.
[33] Kakac S, Shah R, Aung W. *Handbook of Single Phase Convective Heat Transfer*. New York: Wiley (1987).